

Effect of Heat Treatment on Microstructure and Mechanical properties of high strength low alloy (HSLA) steel

Siyuan ZHAO¹, Kaixuan CHEN¹, Yaliku•WUQIKUN¹, Xiaohua CHEN^{2*}, Zidong WANG^{1*}

1 School of Science and Engineering, University of Science and Technology Beijing, Beijing, China

2 State Key Laboratory for Advanced Metals and Materials, University of Science and Technology Beijing, Beijing, China

***Corresponding Author:** Xiaohua CHEN, State Key Laboratory for Advanced Metals and Materials, University of Science and Technology Beijing, Beijing, 100083, China, chenxh@skl.ustb.edu.cn; Zidong WANG, School of Science and Engineering, University of Science and Technology Beijing, Beijing, 100083, China, wangzd@mater.ustb.edu.cn

Abstract:

In this paper, a Fe-based Mn-Ni-Cr-Mo high strength low alloy (HSLA) steel was prepared by using Vacuum melting, following by hot rolling with 78% deformation and various heat treatment processes. Microstructure were characterized by optical microscope (OM), scanning electron microscope (SEM) equipped with energy dispersive spectrometer. Tensile tests were performed. After direct quenching (Q) from 860°C, the samples were subjected to secondary quenching (L) at different intercritical temperatures within the two-phase region and various tempering temperatures (T). Results show that QLT treatment increases elongation and decreases yield ratio compared with conventional quenching and tempering process (QT). The optimum QLT heat treatment parameter in terms of temperature are determined as Q: 860°C, L: 700°C, and T: 600°C, resulting in the better combined properties with yield strength of 756MPa, tensile strength of 820MPa, tensile elongation of 16.76% and yield ratio of 0.923.

Keywords: high strength low alloy (HSLA) steel; QLT heat treatment; tempering; microstructures; mechanical properties

1. Introduction

In order to meet the development of large-scale, high-speed and multi-sea operations of high strength low alloy (HSLA) steel, a steel system with high strength, high toughness and good weldability to allow reliable operation must be assured for extreme severe environments and service conditions^[1]. This indicate an increasing requirement for HSLA steel. In the decades, researchers have done a lot of works in the field of HSLA steel, for example, widely-used high yield (HY) series high-strength steel in the United States, Japanese NS series steel, and Russian Ab-series steel^[2-8]. Above mentioned traditional HSLA steels are based on low-carbon and low-alloys^[9,10], and their high strength and high toughness is attained based on the low-carbon tempered martensite structure obtained through the “quenching and tempering” heat treatment process. The high strength of steel required higher alloy element content, which simultaneously results enhanced in carbon equivalent and thus the deteriorating welding performance. Therefore, how to balance strength, toughness and welding performance of steel has become a key factor in the development of high strength steel.

New ideas have been provided to achieve strength-toughness-welding performance balance. The United States first proposed a new generation of copper-containing easy-welded high strength submarine steel plan to develop the same strength and toughness index as HY 80 steel^[11,12], with better weldability in comparison with HSLA 80 structural steel. HSLA 80^[13] is a low-carbon, copper-precipitated reinforced steel. The ϵ -Cu precipitation and ultra-fine bainite structure with high density dislocation in the steel yield excellent comprehensive mechanical properties. Through dispersion strengthening of ϵ -Cu phase formed in the aging process, the strength loss caused by C is compensated, and the welding crack sensitivity is reduced^[14].

At present, high strength steel systems of 390MPa, 440MPa, 590MPa and 785MPa have been formed^[15], which all use the Mn-Ni-Cr-Mo component system mostly treated with quenching and tempering. The Mn-Ni-Cr-Mo component system treated with quenching and tempering can meet the requirements of technical indicators, but also has some shortcomings. First of all, after heat treatment of quenching and tempering process

[16-18], yield ratio is relatively high, generally up to 0.93 or more, sometimes even as high as about 0.97, which greatly reduces the safe using performance. Secondly, tempering temperature range is narrower during the quenching and tempering process, which increases the difficulty of industrial production. In this paper, we employed a special heat treatment procedure, named QLT treatment [19] which consists of direct quenching (Q), relatively low temperature (intercritical) quenching (L) and tempering (T) to improve the mechanical properties and modify the microstructure of HSLA steel, respectively [20]. The microstructure is refined and ferrite is introduced on the basis of the strengthened phase (tempered martensite) during this heat treatment process. Recently, it has been recognized that the multi-phase microstructure which consists of “soft” ferrite/pearlite and “hard” bainite/martensite would improve the impact property of the steel [21,22]. The combination of soft ferrite and relatively hard secondary tempering martensite reduces the yield ratio and improves elongation. In this paper, a low carbon alloy steel containing alloying elements Ni, Cr, Mo, etc. in hot-rolled state was experienced QT and QLT treatments in sequence. The effects of conventional quenching and tempering heat treatment process (QT) and two-phase zone secondary quenching heat treatment process (QLT) on the microstructure and mechanical properties of the steel were investigated and compared. The results show that QLT heat treatment process improves the elongation and reduces yield ratio obviously.

2. Experimental Procedures

2.1. Preparation of samples

The steel sample with chemical compositions (see Table 1) similar to Mn-Ni-Cr-Mo HSLA steel was prepared. Steel ingot of 150 mm length, 70 mm width and 80 mm thickness was obtained by melting the mixture of all base metals in a corundum crucible in a vacuum furnace [23]. Before melting, degreasing, rust removal and drying treatment

were applied to reduce the introduced inclusions and gas. Vacuum deaeration was adopted and the system vacuum degree is 6×10^{-4} Pa. Oxygen level was controlled in a reasonable range of 40–60 ppm in the melt and nitrogen level in a range of 10–20 ppm. Finally, the melt was poured and cooled down inside the crucible in air. Fabrication process has been presented in detail in our former paper [24].

Then, as-cast ingots were heated at 1200 °C for 2 h and subjected to hot-rolling into 18 mm thick plates with a total cumulative reduction of 78% given in five passes, followed by air cooling to room temperature. By using far-infrared instrument, initial and final rolling temperatures were measured to be 1150 ± 10 °C and 850 ± 10 °C, respectively. Hot-rolled sample of 510 mm length, 105 mm width and 18 mm thickness was then cut into blocks by wire cut electrical discharge machining (WEDM). The sample after hot rolling is divided into two groups named I and II. Group I blocks of rolled-steel with size of 110 mm length, 30 mm width and 10 mm thickness were kept at 880 °C, 860 °C and 840 °C for 1 h quenched in water and subsequently tempered at temperatures of 600 °C for 1h. Group II are after direct quenching from 860 °C, the samples were subjected to secondary quenching (L) at different intercritical temperatures within the two-phase region and various tempering temperatures (T). The QLT treatment includes two step quenching and tempering. Table 2 illustrates the treatment processes used in this paper. The QLT process adds a two-phase zone quenching process between the QT processes. The measured AC1 temperature is 706 °C, and the AC3 temperature is 767 °C. For the QLT processing here, the selected heated temperature is set between 680 °C -760 °C, which is actually high tempering temperature. But the water quenching is chosen as the cooling method, instead of air cooling or furnace cooling. So we called this special processing as a kind of secondary quenching. Therefore, the secondary quenching temperature range is 680-760 °C.

Table 1. Actual chemical compositions of steels (wt.%).

Composition	C	Si	Mn	P	S	Cr	Ni	Cu	Mo	V	Nb	Al
Content	0.06	0.04	1.03	0.02	0.02	0.97	4.66	0.02	0.54	0.003	0.05	0.002

Table 2. The treatment processes of steel.

Name	1	2	3	4	5	6	7	8
Primary quenching temperature	860 °C ×1h							
Secondary quenching temperature	760 °C ×1h	730 °C ×1h	700 °C ×1h	680 °C ×1h	700 °C ×1h	700 °C ×1h	700 °C ×1h	700 °C ×1h
Tempering temperature	600 °C ×1h	600 °C ×1h	600 °C ×1h	600 °C ×1h	640 °C ×1h	620 °C ×1h	600 °C ×1h	580 °C ×1h

2.2. Material characterization and mechanical property test

Optical microscopy (OM), scanning electron microscopy (SEM), equipped with energy dispersive spectrometer

were performed to characterize the microstructures. The spot resolution for the energy dispersive spectrometer (EDS) analysis is 0.205 nm. Metallographic specimens were ground with silicon carbide paper and subsequently polished followed by etching with 4% alcohol nitric acid

solution. Tensile test specimens were cut from hot-rolled samples and tempered samples with WEDM, respectively. Tensile tests were conducted on dog-bone shaped specimens with a gage size of 30mm length, 12.5mm width and 2mm thickness at room temperature with a strain rate of 10–3s–1 using an FPZ 100 machine. The hardness test is conducted on the WHR-80D total Rockwell Hardness tester. The hardness of the experimental steel in rolled and heat-treated state is measured according to the GB/T 2850-1992. 6 points were measured at different positions on the metallographic samples with 10mm×10mm×10mm, and then the average value was obtained as the hardness for the tested samples.

3. Results and Discussion

3.1. Effect of QT process on microstructure and mechanical properties

Figure 1 and Figure 2 show the optical microscope images and scanning electron micrographs of the microstructure at different quenching temperatures. The steel in QT state exhibited a tempered troostite structure in temper state, with quenching at 840°C, 860°C, 880°C and tempering at 600°C. Most of the martensite structure in the troostite structure remained in slat-like shape as shown in SEM images of these QT steels. Numerous carbides were precipitated between martensite slats and at grain boundaries of original austenite. The tempering stability is improved due to the presence of strong carbide forming elements such as Mo, V, Nb, etc. Therefore, most of tempering microstructure

maintains the form of slat, accompanied with high strength.

Quenching temperature influences directly the grain size of austenite structure and correspondingly affects the distribution of quenching structure, leading to the variation of tempering structure (see Fig. 2). Specifically, the higher quenching temperature, the coarser structure in austenitizing (austenite grain), quenching (lath martensite) and tempering (tempering troostite) states. The final tempering structure causes the difference in mechanical properties (see Table 3). On the other hand, the experimental steel contains alloying elements including Ni, V, Cr, and Mo. As the quenching temperature increases, the solid solution contents of the alloying elements increase in the quenching state, which facilitate the precipitation of carbides and nitrides during tempering process. This makes a great contribution on the improvement of strength. The mechanical testing results in Table 3 demonstrate that increase of quenching temperature has the greatest impact on the decline of the yield and tensile strengths of steel. With quenching temperature increasing, specifically, tensile strength decreased from 1055MPa to 908MPa, and yield strength decreased from 882MPa to 878MPa. Tensile elongation and yield ratio at different QT states exhibit similar values around 13% and 0.96, respectively. Therefore, considering several mechanical properties parameters, we conclude that the steel quenched at 860°C and tempered at 600°C obtain the optimized comprehensive mechanical properties, with the yield strength of 881MPa, tensile strength of 909MPa, elongation after fracture of 13.92 %, and yield ratio of 0.969.

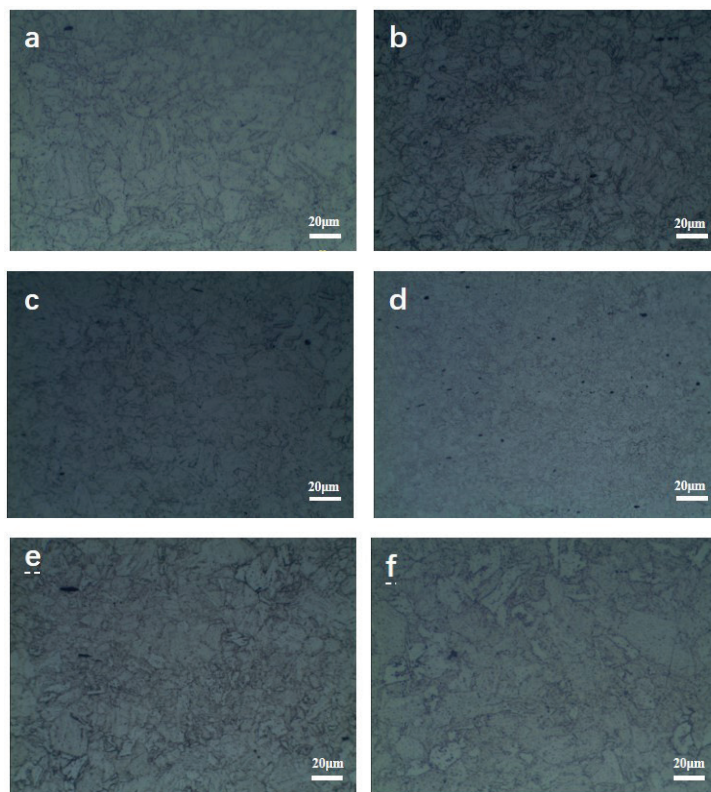


Figure 1. Low magnification optical micrographs of tempered samples at different quenching temperature. Quenching temperature: (a) 840°C; (b) 840°C; (c) 860°C; (d) 860°C; (e) 880°C; (f) 880°C. Tempering temperature: 600°C.

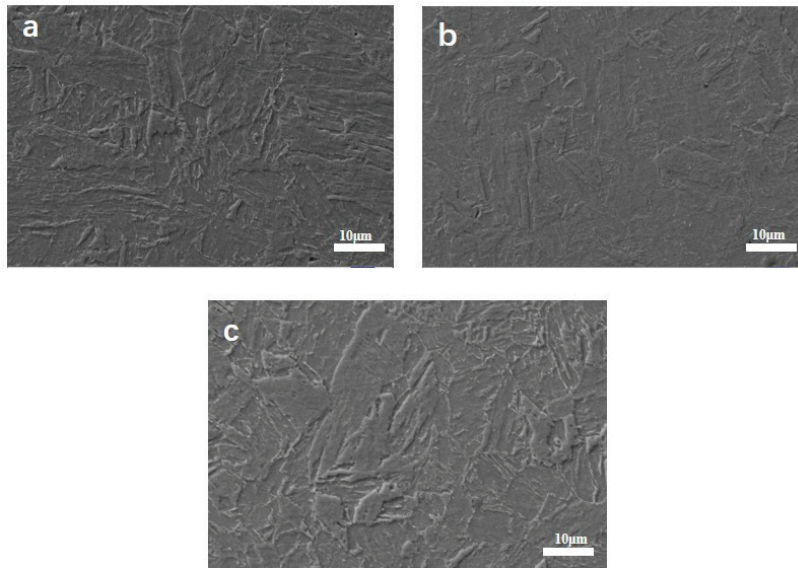


Figure 2. SEM images of at different quenching for 1h and tempering at 600°C, (a) 840°C; (b) 860°C; (c) 880°C

Table 3. Mechanical performance of QT state steel

number	quenching (°C)	temper (°C)	Yield Strength (MPa)	tensile strength (MPa)	Elongation (%)	hardness (HR)	Yield ratio
A	Rolled state	600	0	1055.514	12.16	29.7	0
B	880	600	878.813	908.8632	13.6	28.7	0.967
C	860	600	881.063	909.2028	13.92	26.9	0.969
D	840	600	882.121	910.853	13.84	27.3	0.968

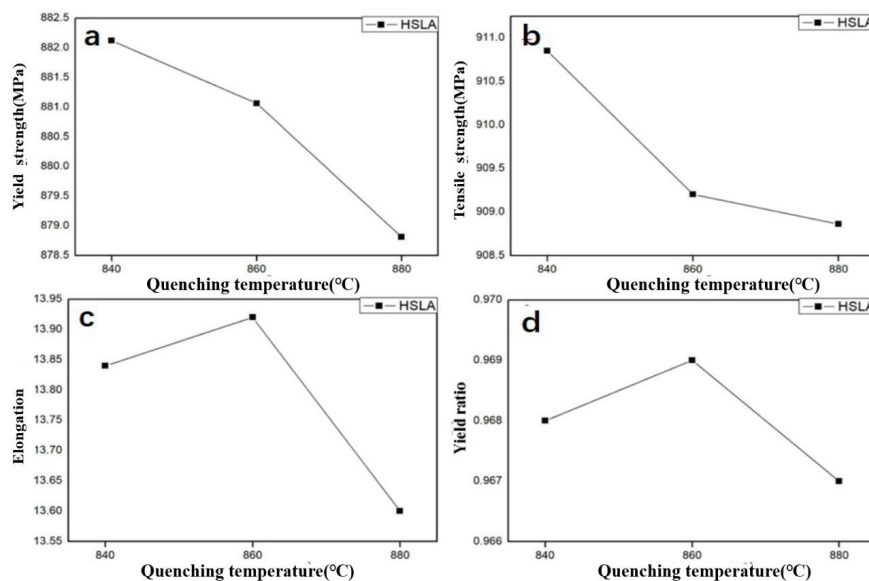


Figure 3. Evolution of mechanical properties with different quenching temperatures: (a) Yield strength; (b) Tensile strength; (c) Elongation; (d) Yield ratio

3.2. Effect of QLT process on microstructure and mechanical properties

In the previous stage, the effects of different quenching temperatures on the microstructure and properties of

steel were investigated. The optimum QT heat treatment parameter in terms of temperature are determined as Q: 860°C and L: 600°C, resulting in the better combined properties with yield strength of 881MPa, tensile strength

of 909MPa, tensile elongation of 13.92% and yield ratio of 0.969. The secondary quenching process was conducted to further verify the relevant properties of the experimental steel.

The secondary quenching produces the continuous distribution of the mixed structure of the secondary tempered martensite and ferrite, similar as the dual-phase steel structure. The combination of the soft ferrite and the hard secondary tempered martensite has the greatest impact on the decline of the yield ratio and the increase of the elongation. Table 4 gives detailed parameters of mechanical properties under different secondary quenching processes (i.e. QLT states). With the secondary quenching temperature increasing, specifically, tensile strength increased from 802 MPa to 912MPa, and yield strength increased from 740MPa to 887MPa. At different QLT states, tensile elongation exhibit similar values around 16%, and yield ratio is higher than 0.89.

Considering the mechanical properties in Table 4, processed in sequence by the quenching at 860°C, secondary quenching at 680-760°C and tempering at 600°C, the steel under 700°C secondary quenching obtain

the optimized comprehensive mechanical properties, with the yield strength of 756MPa, tensile strength of 820MPa, elongation after fracture of 16.96 %, and yield ratio of 0.923.

Then under the constant secondary quenching temperature of 700°C, tempering processes at 580°C, 600°C, 620°C, 640°C for 1 h were carried out to determine the best tempering temperature for the steel. After the secondary quenching and high temperature tempering (>500°C), the obtained microstructure displayed a ferrite+ secondary tempered martensite. When residual austenite is present in the quenched steel, it can even be transformed into pearlite or bainite during tempering and then martensitic transformation occurs. The austenite does not decompose in the tempering heat preservation. In the subsequent cooling, due to the catalysis (anti-stabilization) effect, it is likely to undergo martensitic transformation. This phenomenon is called secondary quenching. Then the structure obtained when tempering is secondary tempered martensite. As the tempering temperature increases, the ferrite content increases and the distribution areas becomes wider (see Fig. 4).

Table 4. Mechanical performance of QLT state steel

Secondary quenching temperature (°C)	Temper temperature (°C)	Yield Strength (MPa)	tensile strength (MPa)	Elongation (%)	Yield ratio
760	600	887.212	912.152	15.20	0.972
730	600	861.354	907.652	16.40	0.949
700	600	756.862	820.498	16.96	0.923
680	600	740.251	802.513	17.20	0.893

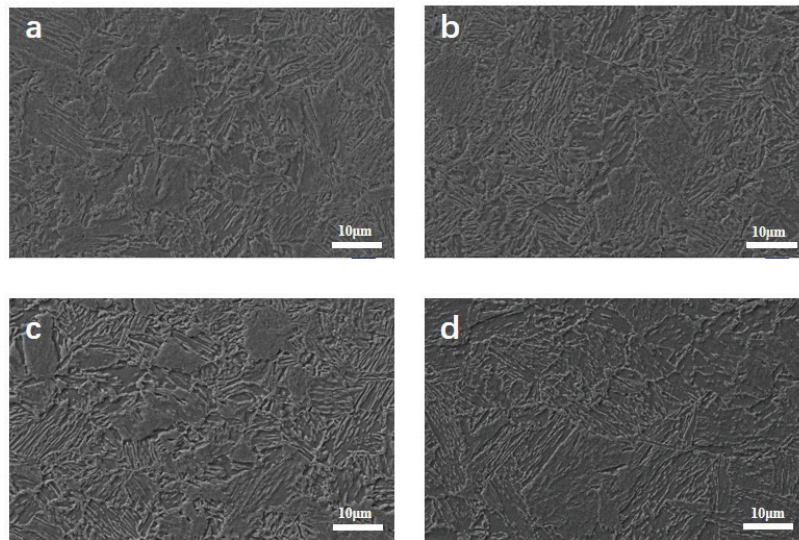


Figure 4. SEM images of at Secondary quenching 700°C for 1h and different tempering (a) 580°C; (b) 600°C, (c) 620°C, (d) 640°C

With the temper temperature increasing, specifically, tensile strength decreased from 846MPa to 787MPa, and yield strength decreased from 785MPa to 700MPa. At different QLT states, tensile elongation decreased

first and then rose, between 16.96-19.60, and yield ratio exhibited similar values around 0.93 (in Table 5 and Fig. 5). Considering the mechanical properties processed in sequence by the quenching at 860°C, secondary quenching

at 700 °C and tempering at 580-640 °C, the steel tempering at 600 °C obtained the optimized comprehensive mechanical properties.

The tensile fracture surfaces of the experimental steel after the QT and QLT process are shown in Figs. 6 and 7. The number density and depth of dimples in fracture surface of steel sample quenching at 840 are less and smaller than those at 860 °C, respectively. Besides, the number density

and depth of dimples in fracture surface of steel sample tempered at 580 °C are less and smaller than those at 600 °C, respectively. The toughness of steel sample quenching at 860 °C (during QT process) and tempered at 600 °C (during QLT process) respectively present higher values compared to their counterparts, which is consistent with the previous reports that dense and deep dimples during tensile fracture induce higher toughness [26,27].

Table 5. Mechanical properties of QLT Process steel

	Secondary quenching temperature (°C)	Temper temperature (°C)	Yield Strength (MPa)	tensile strength (MPa)	Elongation (%)	hardness (HR)	Yield ratio
1	700	640	700.43	787.020	19.60	22.2	0.890
2	700	620	765.16	814.232	19.28	23.4	0.940
3	700	600	756.86	820.498	16.96	23.1	0.923
4	700	580	785.10	846.560	18.16	22.9	0.928

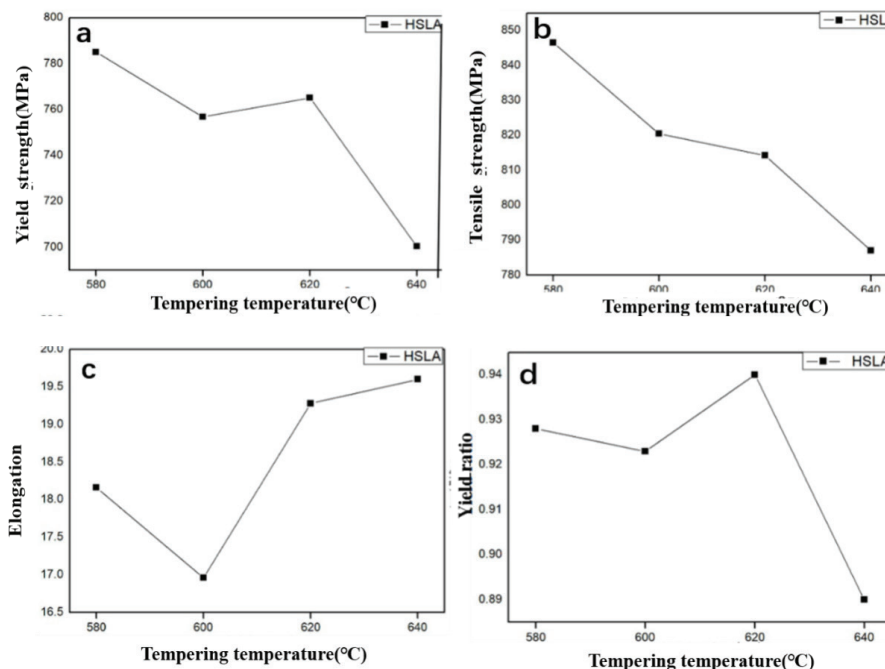
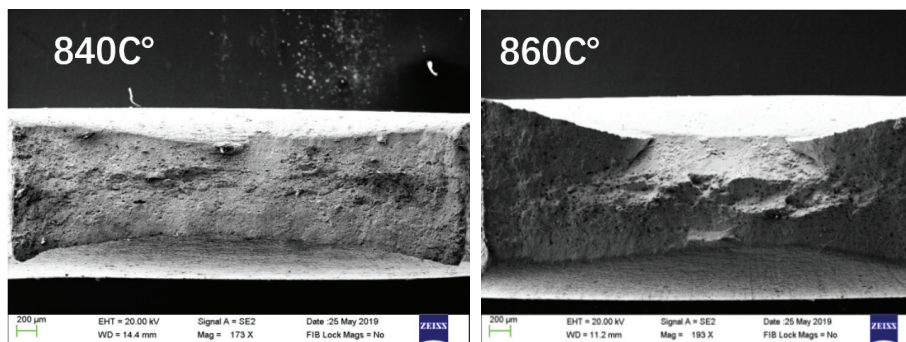


Figure 5. Mechanical properties of different tempering temperatures at 700 °C secondary quenching (a) Yield strength (b) Tensile strength (c) Elongation (d) Yield ratio



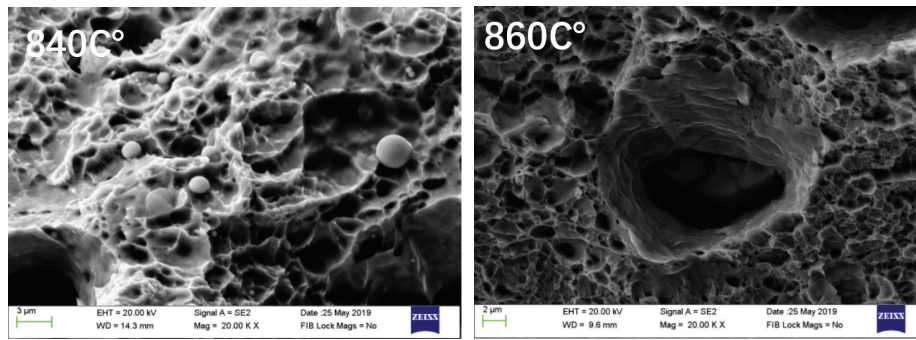


Figure 6. Fracture surface of steel sample quenched at 840 and 860 °C

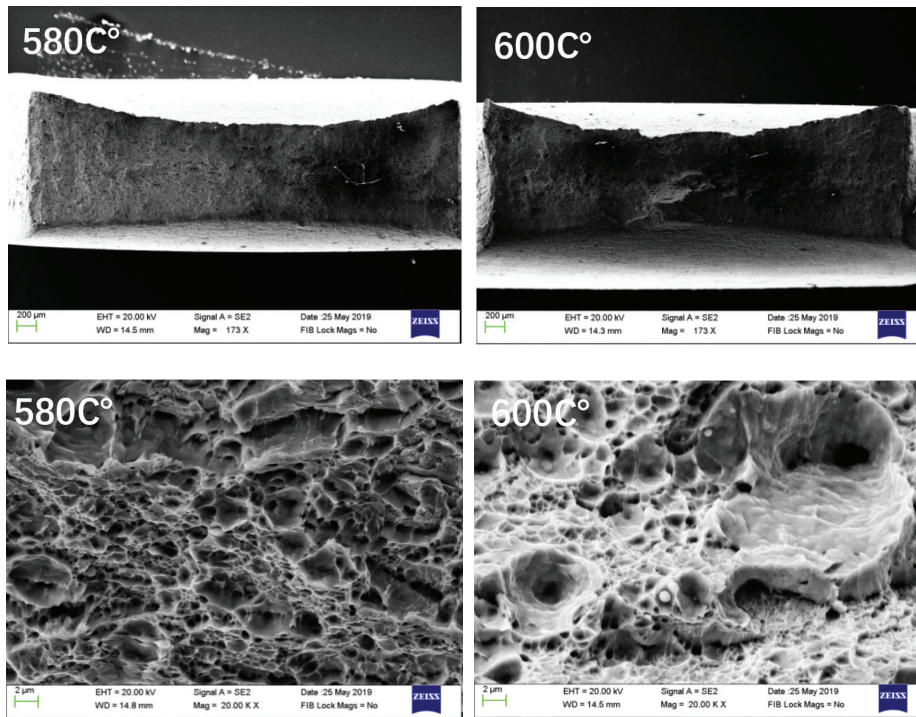


Figure 7. Fracture surface of steel sample tempered at 580 and 600 °C, following secondary quenching at 700 °C

4. Conclusion

(1) Metallographic structure under QT state is mainly consisted of tempered troostite in slat form. The steel under QT state (quenching at 860°C and tempering at 600°C) obtains the optimized comprehensive mechanical properties, with the yield strength of 881 MPa, tensile strength of 909MPa, elongation after fracture of 13.92 %, and yield ratio of 0.969.

(2) The QLT treatment gives the best elongation values compared with QT process, and the optimum QLT heat treatment parameters are determined as Q: 860 °C, L: 700 °C and T: 600 °C, with the yield strength of 756MPa, tensile strength of 820MPa, elongation after fracture of 16.76 %, and yield ratio of 0.923. After QLT treatment, the two-phase structure is formed with soft ferrite and hard tempered martensite, which degrades yield ratio and improves elongation.

(3) The tensile fracture surfaces of the QT and QLT

steels show that the number density and depth of dimples quenching at 840°C (during QT process) and tempered at 580°C (during QLT process) are less and smaller than those of their counterparts, respectively. The dense and deep dimples during tensile fracture induce higher toughness in the former steels.

Acknowledgments: This work was supported by the Project funded by China Postdoctoral Science Foundation, the Fundamental Research Funds for the Central Universities (No. FRF-TP-19-002A1), Domain Foundation of Equipment Advance Research of 13th Five-year Plan (No. 61409220124).

References

- [1] Czyryca, E.J. Advances in High Strength Steel Technology for Naval Hull Construction. Key Eng. Mater. 84–85, 491–520.

- [2] Jun Shao. Research status and development of ship steel [J]. *Angang Technology* 2013, (04), 1-4.
- [3] Wenkui Hao; Zhiyong Liu; Xianzong Wang; Xiaogang Li. The current status and development trend of strength and corrosion resistance of high-strength steel for ships [J]. *Equipment Environmental Engineering* 2014, 11 (01), 54-62.
- [4] Shike Yin, Changhong He, Yalin Li. Submarine steel and its welding materials in the United States and Japan [J]. *Materials Development and Application* 2008, (01), 58-65.
- [5] Heng Ma, Zhonghua Li, Xiaobo Zhu, et al. Development status of thick steel for aircraft carrier [J]. *Shandong Metallurgy* 2010, 32 (2), 8-10.
- [6] Xiaoyan Huang, Bo Liu. Structural materials for ships current status and development [J]. *Ship & Boat* 2004, (3), 21-24.
- [7] Shidong Wu. Development and Application of Structural Steel for U.S. Ships Study [J]. *Shanghai Shipbuilding* 2006, (4), 57-60.
- [8] Xin'an Cheng. Review and Prospect of Overseas Ship Steel [J]. *Development and Application of Materials* 1997, 12 (2), 46-48.
- [9] Chen X Z, Huang Y M. Microstructure and properties of 700MPa grade HSLA steel during high temperature deformation [J]. *Journal of Alloys and Compounds* 2015, 631:225-231. Fernandez J, Illesca S S, Guilemany J M. Effect of microalloying elements on the austenitic grain growth in a low carbon HSLA steel [J]. *Materials Letters* 2007, 61 (11), 2389-2392.
- [10] Fernandez J, Illesca S S, Guilemany J M. Effect of microalloying elements on the austenitic grain growth in a low carbon HSLA steel [J]. *Materials Letters* 2007, 61 (11), 2389-2392.
- [11] Heller S R, Friti I, John V. An evaluation of HY-80 steel as a structural material for submarine, Part I [J]. *Naval Engineering Journal* 1965, (2).
- [12] Heller S R, Friti I, Vasta J. An evaluation of HY-80 Steel as a structural material for submarine Part II [J]. *Naval Engineering Journal* 1965, (4).
- [13] Katsumata M, Ishiyama O, Inoue T. Microstructure and Mechanical Properties of Bainite Containing Martensite and Retained Austenite in Low Carbon HSLA Steels 1991(08).
- [14] S D, A G, S C. Microstructural characterization of controlled forged HSLA-80 steel by transmission electron microscopy [J]. *Materials Characterization* 2003, 50 (4-5), 305-315.
- [15] The State-of-Art and Development Trends of HSLA Steels in China [J]. *Journal of Iron and Steel Research* 2011, 18 (S1), 1-13.
- [16] Yuan G. Kang J, Zhaodong W, Guodong W. Effect of Heat Treatment on Microstructure and Mechanical Properties of HSLA Plate Steel [A]. Chinese Society for Metals. Proceedings of the 10th International Conference on Steel Rolling [C]. 2010; 4.
- [17] Chaudhury Z A, Sarma D S. Influence of Heat Treatment on Structure and Properties of a HSLA Steel, 1982; (02).
- [18] Bai D Q, Yue S, Maccagno T M. Effect of Deformation and Cooling Rate on the Microstructures of Low Carbon Nb-B Steels, 1998; (04).
- [19] S.J. Wu, G.J. Sun, Q.S. Ma, Q.Y. Shen, L. Xu. Influence of QLT treatment on microstructure and mechanical properties of a high nickel steel [J]. *Journal of Materials Processing Tech* 2013, 213 (1).
- [20] Yongchang Liu, Lei Shi, Chenxi Liu, Liming Yu, Zesheng Yan, Huijun Li. Effect of step quenching on microstructures and mechanical properties of HSLA steel [J]. *Materials Science & Engineering A* 2016, 675.
- [21] M.R. Akbarpour, A. Ekrami, Effect of Ferrite Volume Fraction on Workhardening Behavior of High Bainite Dualphase (DP) Steels, *Mater. Sci. Eng.:* A477, 2008; 306-310.
- [22] R. Bakhtiari, A. Ekrami, The Effect of Bainite Morphology on the Mechanical Properties of a High Bainite Dualphase (HBDP) Steel, *Mater. Sci. Eng.:* A525, 2009; 159-165.
- [23] Yasong Li, Ruixuan Li, Yong Zhang. Effects of Si Addition on Microstructure, Properties and Serration Behaviors of Lightweight Al-Mg-Zn-Cu Medium-entropy Alloys [J]. *Research and Application of Materials Science* 2019, (01), 13-22.
- [24] Xiaohua Chen, Lili Qiu, Hao Tang, Xiang Luo, Longfei Zuo, Zidong Wang, Yanlin Wang. Effect of nanoparticles formed in liquid melt on microstructure and mechanical property of high strength naval steel [J]. *Journal of Materials Processing Tech.*, 2015, 223-224
- [25] Tang, H., Chen, X.H., Chen, M.W., Zuo, L.F., Hou, B., Wang, Z.D., Microstructure and Mechanical Property of In-situ Nano-particle Strengthened Ferritic Steel by Novel Internal Oxidation, *Mater. Sci. Eng.* 2014; A 609, 293-299.
- [26] Ruiyang Wang, Shiqing Sun, Song Wang, Nianlun Wei, Boshuai Cui. Analysis of M50 bearing steel turning bend fracture [J]. *Internal Combustion Engines and Parts* 2019, (04), 61-62.
- [27] Kai Feng, Daming Jiang, Bande Hong. Fracture Analysis of Low Carbon Duplex Steel [J]. *Materials for Mechanical Engineering* 1992, (03), 58-61.